

# Modification of Silk Fibroin and Gelatin-Chondroitin Sulfate Matrix with the Addition of Nanohydroxyapatite by Freeze-Drying Method for Tissue Engineering Application

Mohammad Azadi<sup>1\*</sup>, Zahra Shams Ghahfarokhi<sup>2</sup> and Abbas Teimouri<sup>1</sup>

<sup>1</sup> Department of Chemistry, Payame Noor University, P. O. Box 19395-3697, Tehran, Iran.

<sup>2</sup> University of Birjand, Birjand, I. R. of Iran.

Received: 12 May 2017, Revised: 3 Aug. 2017, Accepted: 4 Aug. 2017.

Published online: 1 Sep. 2017.

**Abstract:** Silk fibroin/gelatin-chondroitin sulfate/nanohydroxyapatite (SF/GE-CS/nHAp) composite scaffolds were prepared by freeze-drying approach. The prepared samples were investigated using BET, FTIR, SEM, and XRD studies. In addition, the investigation of the cell proliferation, adhesion and viability using MTT, DMEM solution, and mouse preosteoblast cell confirmed the cytocompatible nature of the composite scaffolds. These results showed that this composite could be a potential candidate for tissue engineering application.

**Keywords:** Chondroitin sulfate, Nanohydroxyapatite, Nanocomposite scaffolds, Gelatin, Silk fibroin, Tissue engineering.

## 1 Introduction

Tissue engineering attempts to develop biological substitutes for damaging organs and tissues. It has been applied to develop a cell-based material for bone healing, which is established on scaffolds used to support and strengthen [1]

Natural bone is a complex inorganic organic nanocomposite material in which collagen fibrils and nHAp nanocrystals are embedded within collagen fibrils [2] Nanohydroxyapatite is an osteoconductive, non-toxic and non-inflammatory biomaterial. The problems associated with nHAp ceramic, such as intrinsic fragileness, migration of nHAp particles from the implanted sites and poor formability can be improved by the adhesion of nHAp ceramic with biopolymers such as silk fibroin and gelatin [3,4]. Gelatin, a biocompatible protein, is a partially degraded product of collagen. Gelatin has been incorporated into scaffolds to promote cell migration, adhesion, differentiation and proliferation [5].

Chondroitin sulfate is arranged in repeating disaccharide units consisting sulfate ester and carboxylic groups in which the positively charged growth factors can be

connected [6]

Silk fibroin has been widely studied due to its promising properties such as high tensile strength, controllable biodegradability, haemostatic properties good biocompatibility, non-cytotoxicity, non-inflammatory, low immunogenicity and excellent

Mechanical properties and biochemical features [7] in continuation of our recent study on the construction of composite scaffolds [8-15] in this work, we focus on the preparation, characterization, bioactivity, biodegradation and mechanical and in vitro properties of nano-composite scaffolds SF/GE-CS/nHAp in detail.

## 2 Experimental

### 2.1 Materials

Raw cocoons of silkworm, *Bombyxmori*, prepared from a sericulture farm in Natanz, Iran. Chondroitin sulfate (sodium salt from shark cartilage) and other agents were purchased from Sigma-Aldrich. Cellulose dialysis cassettes (Slide-A-lyzer, MWCO 12000 Da (Sigma)) were used. Mouse preosteoblast cell line (MC<sub>3</sub>T<sub>3</sub>-E<sub>1</sub>) was purveyed by

\*Corresponding author E-mail: [mohammad\\_azadi60@yahoo.com](mailto:mohammad_azadi60@yahoo.com)

Riken Cell Bank (Ibaraki, Japan). The MC<sub>3</sub>T<sub>3</sub>-E<sub>1</sub> cells were cultured in low glucose-Dulbecco's modified Eagle's medium (DMEM), with 10% fetal bovine serum (Sigma), 1% penicillin and streptomycin (GIBCO, USA) at 37 °C in a humidified CO<sub>2</sub> incubator.

## 2.2 Preparation of Composite Scaffold

The regenerated silk fibroin and nHAp powder were prepared as described in the literatures [16,17].

Equal the weight of gelatin and chondroitin sulfate were added into the silk solution and stirred for 12 h at 4 °C. Then nHAp was added to the solution and stirred for 24 h to disperse nHAp in the silk solution. Then, 0.25% (v/v) glutaraldehyde was added in 1:32 ratio (2 h) for crosslinking. The resultant solution was transferred to the 24-well culture plates and pre-frozen at -20 °C for 12 h. This was followed by freeze-drying (Dena vacuum industry) at -80 °C for 48 h. The SF content of each specimen was scaled according to the SF/GE-CS/nHAp weight ratios of 15/15/70, 25/25/50, and 35/35/30.

## 2.3 Characterizations

The samples were characterized by X-ray diffraction (Bruker D8ADVANCE, Cu Ka radiation), FTIR spectroscopy (Nicolet 400D in KBr matrix, with the range of 4000-500 cm<sup>-1</sup>), SEM (Philips, XL30, SE detector), Brunauer-Emmett-Teller (BET); Series BEL SORP 18, at -195 °C. The outgas temperature and time are 60 °C and 7 h, respectively.

## 2.4 Porosity, Water-Uptake Capacity and Compressive Strength

The porosity and water-uptake capacity of the scaffolds were measured according to the literatures [8,18]. Compressive strength of the samples was calculated in the dry state at a crosshead speed of 2 mm/min in a material testing 1446-60 machines (Zwick).

## 2.5 Evaluation of Cytotoxicity, Study of Mouse Preosteoblast Cell Proliferation, Mineralization and Degradation in Different SF/GE-CS/nHAp Formulations in Vitro

For in vitro evaluation of cytotoxicity the MTT assay was used as an indicator [19]. Mouse preosteoblast cell line MC<sub>3</sub>T<sub>3</sub>-E<sub>1</sub> was applied to assess the in vitro cytotoxicity of the extractions. Briefly, cells were seeded at seeding densities control groups. The degradation of the SF and (SF/GE-CS/nHAp) composite scaffolds was assayed according to the literature [8] by immersing in a PBS medium at 37 °C for different time intervals (1, 4, 7, 14, 21

and 28 days).

## 2.6 Statistical Analysis

Statistical analyses were performed using SPSS v.16.0 software. Data were expressed as the mean ± significant if  $\rho$  values obtained from the test were less than 0.05 ( $\rho < 0.05$ ).

## 3 Results and Discussion

The morphology of the samples was investigated by SEM. In the scaffolds, forming networks of open and interconnected pores could promote fluid exchange and native tissue ingrowth. In the presence of nHAp, pore walls were rough. They could be, therefore, advantageous for cell attachment (Figures 1a, b, c).

XRD patterns for the samples are shown in Figure 1d. The peaks of the synthesized nHAp particles corresponded to the characteristic XRD spectrum of HAp (JCPDS File No. 09-0432). Many sharp diffractions corresponded to (211), (112), (300), (002), (213), (222), (202), (310), and characteristic XRD spectrum of HAp (JCPDS File No. 09-0432). Many sharp diffractions corresponded to (211), (112), (300), (002), (213), (222), (202), (310), and (321) reflections of nHAp crystal, respectively. These were of a typical apatite crystal structure. The sharp diffraction proved that nHAp was composed of well-developed crystals.

The XRD patterns of the composites simultaneously exhibited the characteristic peaks of nHAp, random coil and silk II structure [20]. In 30% nHAp incorporated scaffolds, the peaks had intensities less than the higher concentration of nHAp.

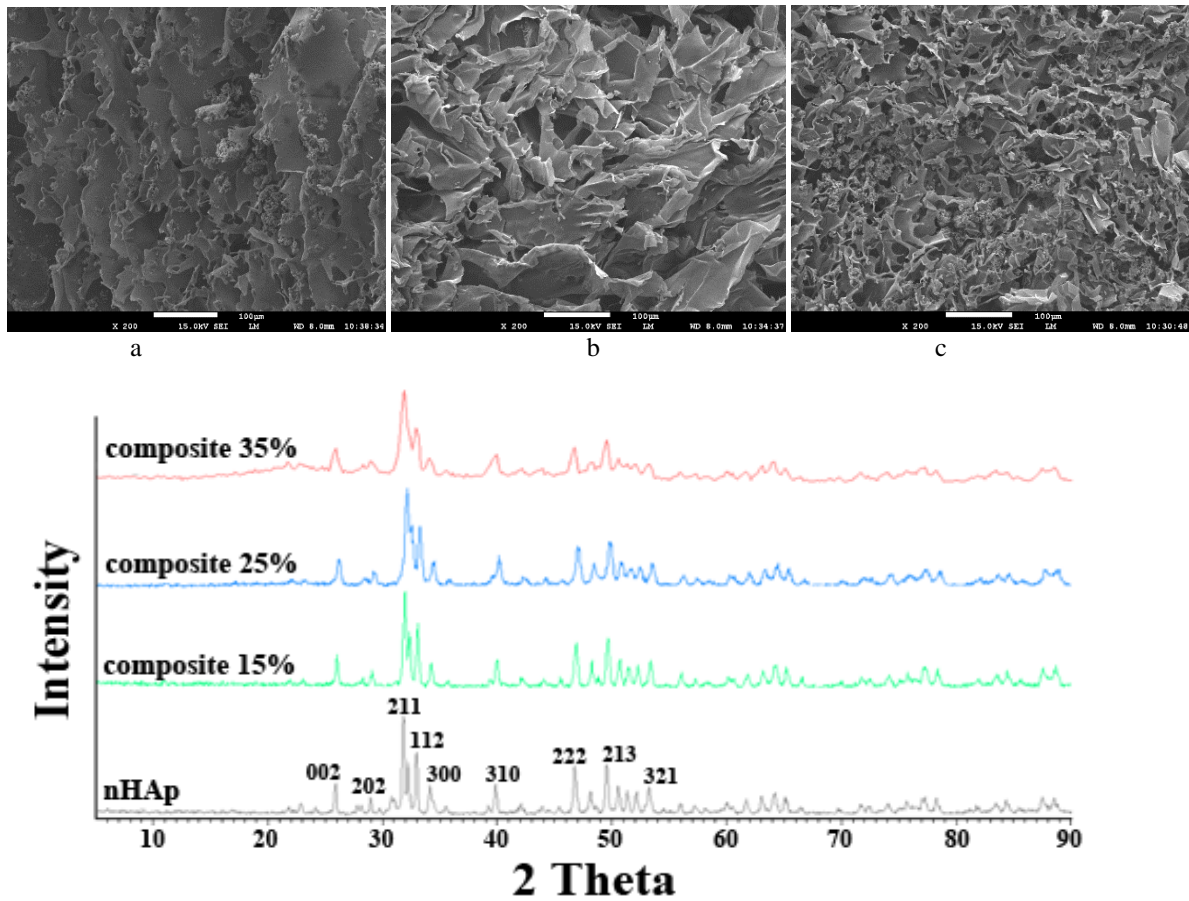
The three nanocomposites display the peaks at the similar position, assigned only to monophase crystalline nHAp, since no diffraction peaks from other calcium phosphate phases are observed. This implies that the addition of GE-CS and SF did not change the crystalline structure of nHAp. The XRD patterns show a preferential growth of nHAp crystallites along c-axis in all three nanoparticles, since the intensity of (002) peak is higher than that of (300) peak [11,12].

Figure 2a displays FTIR peaks of samples. FTIR spectrum of nHAp showed peaks at 632 and 3430 cm<sup>-1</sup>, which were related to -OH bending and stretching vibration mode. The bands at 602 and 567 cm<sup>-1</sup> were related to  $\gamma_4$  of phosphate. The one at 963 cm<sup>-1</sup> and the other at 1042 cm<sup>-1</sup> referred to  $\gamma_1$  and  $\gamma_3$  of the phosphate respectively [21].

The -COOH group of gelatin and chondroitin sulfate in the composite scaffold was in the form of COO<sup>-</sup> and the ionic interaction could exist between Ca<sup>2+</sup> and COO<sup>-</sup> [6, 22]. The absorption bands at 1531 and 1242 cm<sup>-1</sup> could be attributed to the amide II and amide III of SF in SF/GE-CS/nHAp composite scaffolds [16].

Moreover, the band at 1636 cm<sup>-1</sup> corresponded to the absorption of OH group of nHAp, which was observed as a sharper peak at 1630 cm<sup>-1</sup> in SF/GE-CS/nHAp composite

scaffolds, presumably due to the overlap of the bands of OH group in nHAp and amide I in SF. The N<sub>2</sub> adsorption-desorption isotherms of SF/GE-CS/nHAp sample are represented in Figure 2b. The specific area has been calculated by using BET method.



**Figure 1.** SEM images of (a) composite 15%, (b) composite 25%, and (c) composite 35%, (d) XRD patterns of samples.

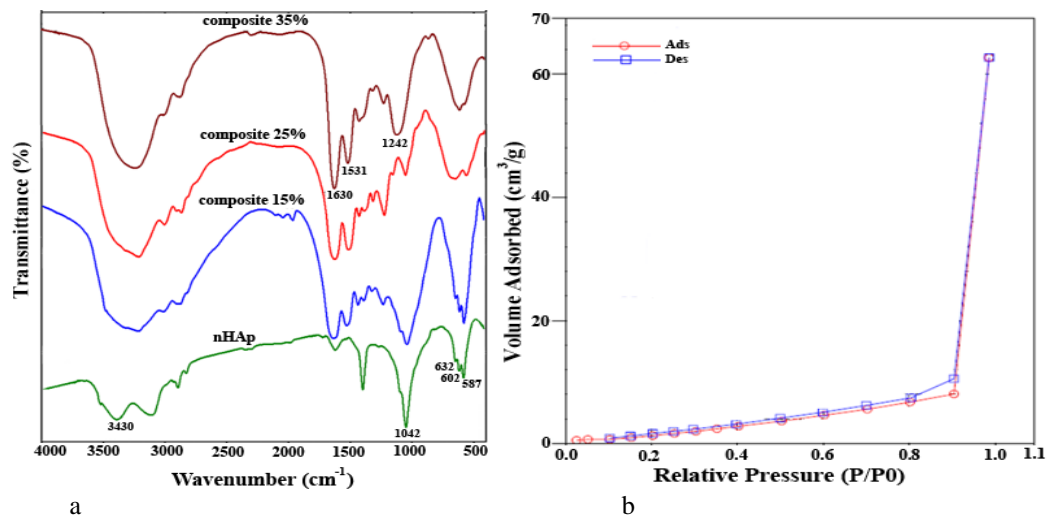


**Figure 2.** (a) FTIR of samples and (b) N<sub>2</sub> adsorption – desorption isotherm of composite 15%.

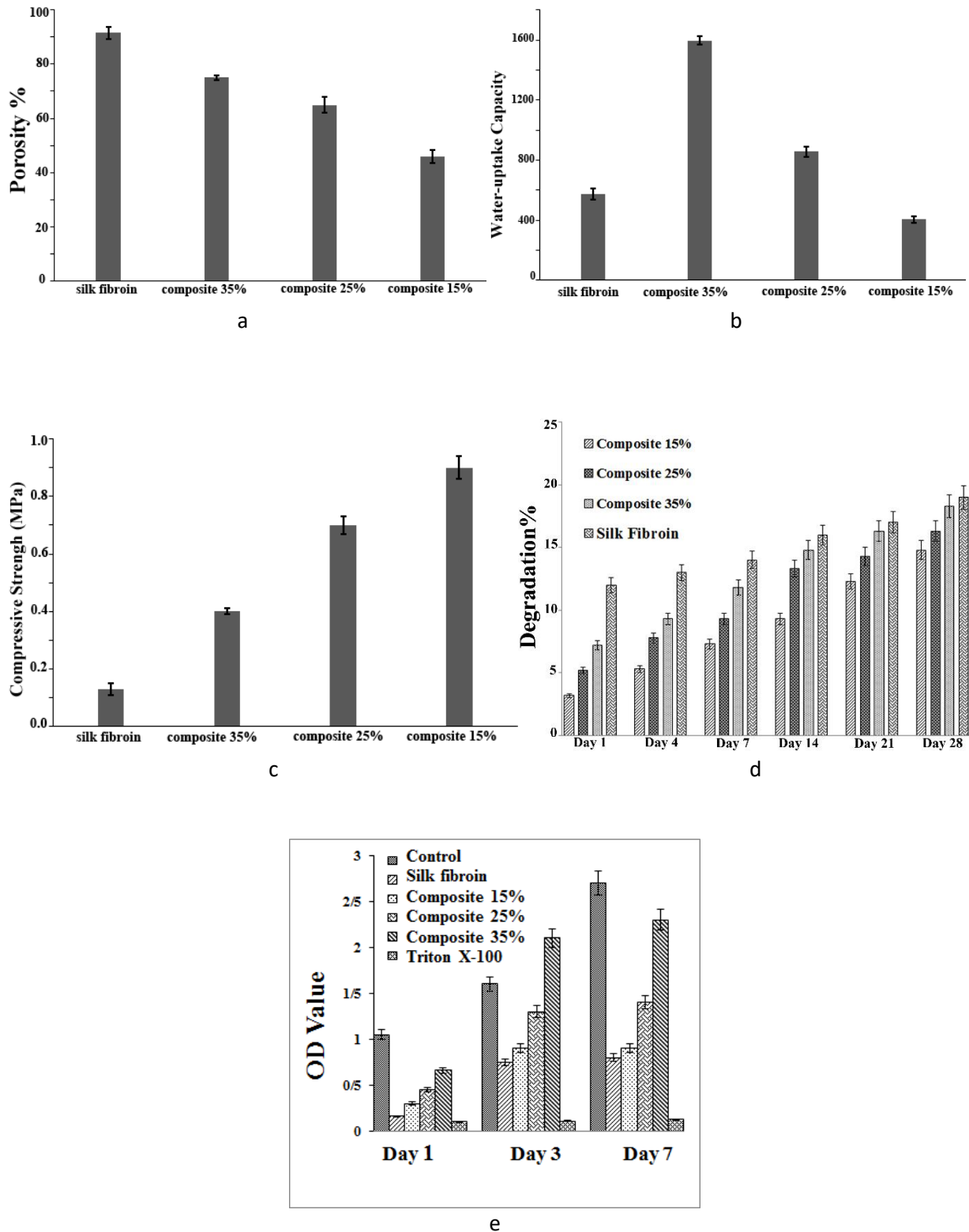


**Figure 3.** (a) Porosity values, (b) Water-uptake values, (c) Compressive strength, (d) Degradation behavior vs time curve of SF and composite scaffolds, (e) In vitro cytotoxicity evaluation of MC<sub>3</sub>T<sub>3</sub> cells in contact with scaffolds for different periods of time.

H3-type hysteresis loops, according to the IUPAC classification. This is known as a characteristic of porous materials with highly uniform size distributions [23]. From the two branches of adsorption-desorption isotherms, the presence of a sharp adsorption step in the P/P0 region from 0.9 to 1.00 and a hysteresis loop at relative pressure greater P/P0 than 0.8 illustrated that the materials processed a well-defined and regular array of porous materials. Also, the measured P/Po points as a function of V adsorbed (cm<sup>3</sup>/g) are in accordance with each other in the P/P0 region from 0.9 to 1.00. The structure data of sample showed that SF/GE-CS/nHAp had a high BET surface area (16.615 m<sup>2</sup>/g) and a large pore volume (0.101 cm<sup>3</sup>/g) indicative of its potential applications the maximum cell growth by adhesion to the scaffold surfaces.

The porosities of the prepared scaffolds are shown in Figure 3a. When the content of SF was increased from 15 to 35 wt.%, the porosities were increased from about 45% to 60%. Cells could travel through the pores and get attached at suitable positions in the scaffold for further proliferation [16]. Water-uptake studies of samples showed in Figure 3b. The addition of SF increased the water-uptake of composite scaffolds, because nHAp formed cross-linking hydrophilic NH<sub>2</sub> or COOH groups. Compressive strength of samples presented in Figure 3c. The increase in pore wall thickness and the reduction in pore sizes by the addition of nHAp could be responsible for the high promote cell adhesion, it could lower its mechanical properties. Figure 3d shows the degradation profiles of samples. The percentages of weight loss of all scaffolds were less than polymers were hydrolyzed quickly in the presence of water [24]. For the scaffolds to be used in the tissue engineering, they should be biocompatible. The scaffolds mechanical properties in composite scaffolds, in chondroitin sulfate by grafting phosphate and calcium to chains that decreased the hydrophilicity of gelatin and of composite scaffolds was faster than the pure SF and was decreased with the addition of nHAp. The hydrophilic macromolecular chains of gelatin and chondroitin sulfate comparison to the SF.

However, while the water uptake of scaffolds would the 20% after 4 weeks. The degradation rate should not be toxic to the bone cells. Thus, the scaffold materials were studied by subjecting the cytotoxic to mouse preosteoblast cells. The proliferation of MC<sub>3</sub>T<sub>3</sub>-E<sub>1</sub> cells in contact with the extraction of the scaffolds was evaluated after 1, 3 and 7 days of culture period by means of MTT test (Figure 3e). The addition of SF (with the decrease in the amount of nHAp) increased the cell proliferation of SF/GE-CS/nHAp composite scaffolds. This could be because of the low crystallinity of nHAp, leading to the dissolution of phosphate and calcium into the media. This, in turn, resulted in the increase in intracellular Ca and phosphate concentration and further induction of the cell death. There were salient differences between days 1, 3 and 7 for all groups. As a positive control, cell incubated with Triton X-100 showed a significant loss of cell viability. The results indicated an obvious increase in cell numbers over time. It was shown that the SF/GE-CS/nHAp composite scaffolds

were cytocompatible, suggesting that these scaffolds were non-toxic to osteoblastic cells.

## 4 Conclusions

The SF/GE-CS/nHAp composite scaffold was found to have good pore size and porosity. The addition of SF increased the cell proliferation of composite scaffolds. The increase in density was related to a decrease in water-uptake and total porosity. It was also shown that nHAp substantially improved cell adhesion on the internal scaffold surfaces. It could be concluded that nHAp played the role of improving the mechanical and biological properties of the scaffolds.

## Acknowledgements

Supports from Payame Noor University Isfahan Research Council (Grant # 84910) and contribution from Isfahan University of Technology are gratefully acknowledged.

## References

- [1] H. S. Kim, J. T. Kim, Y. J. Jung; *Macromol. Res.* 2007, 15, 65-73.
- [2] L. Wang, C. Li; *Carbohydr. Polym.* 2007, 68, 740-745.
- [3] K. Askarzadeh, F. Orang, F. Moztafarzadeh; *Iran. Polym. J.* 2005, 14, 511-520.
- [4] L. Shen-zhou, L. Jia-jia, Y. Shu-qin, L. Jian-bing, L. Ming-zhong; *J. Clinic. Rehabilit. Tissue Eng. Res.* 2009, 13, 6789-6792.
- [5] M. N. Kazemzadeh, F. Orang, M. H. Solati, A. Goudarzi; *Iran. Biomed. J.* 2006, 10, 215-223.
- [6] J. Venkatesan, R. Pallela, I. Bhatnagar, S. Kim; *Int. J. Biol. Macromol.* 2012, 51, 1033-1042.
- [7] L. Ghorbanian, R. Emadi, S. M. Razavi, H. Shin, A. Teimouri; *Int. J. Biol. Macromol.* 2013, 58, 275-280.
- [8] A. Teimouri, L. Ghorbanian, A. NajafiChermahini, R. Emadi; *Ceram. Int.* 2014, 40, 6405-6411.
- [9] A. Teimouri, R. Ebrahimi, R. Emadi, B. Hashemi Beni, A. Najafi Chermahini; *Int. J. Biol. Macromol.* 2015, 76, 292-302.
- [10] A. Teimouri, R. Ebrahimi, A. Najafi Chermahini, R. Emadi; *RSC Adv.* 2015, 5, 27558-27570.
- [11] A. Teimouri, M. Azadi, R. Emadi, J. Lari, A. NajafiChermahini; *Polym. Deg. Stab.* 2015, 121, 18-29.
- [12] M. Azadi, A. Teimouri, G. Mehranzadeh; *RSC Adv.* 2016, 6, 7048-7060.
- [13] A. Teimouri, M. Azadi; *Int. J. Polymer. Mater. Polymer. Biomater.* 2016, 65, 917-927.
- [14] A. Teimouri, M. Azadi, Z. Shams Ghahfarokhi, R. Razavizadeh; *J. Biomater. Sci. Polym. Ed.* 2016, 28, 1-14.

- [15] A. Teimouri, M. Azadi; *Polym. Bull.* 2016, 73, 3513-3529.
- [16] N. Bhardwaj, S. Chakraborty, S. C. Kundu; *Int. J. Biolog. Macromol.* 2011, 49, 260-267.
- [17] C. Stotzel, F. A. Muller, F. Reinert, F. Niederdraenk, J. E. Barralet, U. Gbureck; *Coll. Surf. B: Biointer.* 2009, 74, 91-95.
- [18] R. Nazarov, H. J. Jin, D. L. Kaplan; *Biomacromolecules*, 2004, 5, 718-726.
- [19] J. Li, Y. Dou, J. Yang, Y. Yin, H. Zhang, F. Yao, H. Wang, K. Yao; *Mater. Sci. Eng. C*, 2009, 29, 1207-1215.
- [20] K. S. Katti, D. R. Katti, R. Dash; *Biomed.Mater.* 2008, 3, 034122.
- [21] J. K. Han, H. Y. Song, F. Saito, B. T. Lee; *Mater. Chem. Phys.* 2006, 99, 235-239.
- [22] M. Meskinfam, M. S. Sadjadi, H. Jazdarreh; *Eng. Technol.* 2011, 52, 395-398.
- [23] K. S. W. Sing, D. H. Everett, R. A. W. Haul, L. Moscou, R. A. Pierotti, J. Rouquerol, T. Siemieniewska; *Pure & Appl. Chem.* 1985, 57, 603-619.
- [24] A. P. Marques, R. L. Reis; *Mater. Sci. Eng. C*, 2005, 25, 215-229.